International Journal on Advanced Science Engineering Information Technology

Vol.15 (2025) No. 1
ISSN: 2088-5334

Analysis of Factors Affecting Spectrum Sensing in an IRS based Wireless Network

Mahmoud Zaki Iskandarani [a,*], Rahmat Hidayat [b]

[a] *Faculty of Engineering, Department of Robotics and Artificial Intelligence Engineering Al-Ahliyya Amman University, Amman, Jordan*
[b] *Department of Information Technology, Politeknik Negeri Padang, Padang, Indonesia*
Corresponding author: [*] m.iskandarani@ammanu.edu.jo

Abstract*— Intelligent reflecting surface, or IRS, has shown great promise for wireless networks. IRS provides flexible wireless channel control and setup by dynamically adjusting numerous devices' reflection amplitudes/phase shifts. This dramatically increases the wireless signal transmission rate and dependability. In cognitive radio networks, spectrum sensing and communication security are critical components. Intelligent reflecting surfaces (IRS) to improve the sensing performance and the accuracy of spectrum sensing simultaneously. This work and through MATLAB simulation, carries out analysis of the effect of user traffic (T_{user}), noise factor (N_{factor}), and probability of false alarm (P_{false}) on the ability of an IRS based wireless system to spectrum sense through computation of detection probability ($P_{detection}$). The work provided results, analysis, and mathematical models for both stable and unstable environmental conditions. In addition, two Signal-to-Noise Ratio (SNR) levels are considered, 20% and 80% noise. This enables spectrum sensing to be assessed under different conditions. The results shows that $P_{detection}$ decreases as N_{factor} increases per percentage of T_{user} with a logarithmic shape function. The work also indicates a tenfold increase in the noise factor as the user traffic level goes above 50%. As the noise factor increases for a fixed probability of false alarm, and with user traffic increase, detection probability decreases, and as P_{false} increases, so does the $P_{detection}$. The results indicate that there should be a balance in T_{user} with N_{factor} to optimize $P_{detection}$ and reduce the effect of P_{false} in spectrum sensing.

***Keywords*— Probability; SNR; user traffic; false alarm; detection; noise; IRS; RIS; spectrum sensing.**

Manuscript received 26 Sep. 2024; revised 25 Dec. 2024; accepted 19 Jan. 2025. Date of publication 28 Feb. 2025.

I. INTRODUCTION

The intelligent reflecting surface (IRS) is a novel technique for increasing the effectiveness of wireless communication networks in smart radio environments. It is used to improve the communication qualities of wireless networks. To mitigate the negative consequences of naturally occurring wireless propagation, it alters the scattering, reflection, and refraction of radio waves [1], [2].

In traditional wireless communication systems, data is transferred from a transmitter to a receiver over an erratic propagation environment. Intelligent reflecting surfaces (IRSs) hold great potential for real-time reconfigurable propagation contexts as they may enhance communication rate and expand the number of users served. An IRS is a real-time reconfigurable reflect array that modifies the wireless propagation environment strategically by utilizing a large number of low-cost passive components [3], [4].

With the crucial exception that an IRS uses passive beamforming, which merely permits phase shifts to be applied to the incoming signal and reflects the signal without amplification. The cases for relays and implementing an IRS-assisted system are comparable. Conventional wireless communication systems can function better when IRS-assisted communication is included. Installing an IRS in a structure can have a significant impact on the signal strength and interference attenuation at the receiver side [5], [6], [7].

Effective management of scarce spectrum resources is a critical function of cognitive radio (CR). However, effective spectrum sensing is necessary, using intelligent reflecting surface (IRS) specifically for spectrum sensing. IRS is used to optimize the performance of spectrum sensing. Throughput and spectrum sensing parameters—namely, the likelihood of a false alarm and missed detection—are usually used to assess performance [8], [9].

As wireless communication technology advances, people's need to stay connected to the outside world is growing, which

is forcing us to squeeze a lot of smart wireless devices into a narrow spectrum. This proliferation causes a problem with spectrum shortage. One of the more enticing solutions to the spectrum shortage issue has been cognitive radio. When a licensed or primary user is not using the spectrum, unlicensed or secondary users can access it opportunistically through CR. Spectrum sensing can be utilized to identify the unoccupied area of the spectrum [10], [11].

In cognitive radio networks, spectrum sensing and communication security are critical components. IRS has recently been utilized as a new method to reach the desired spectrum detection probability by using a safe approximation for the Q -function to convert the likelihood of detection into a manageable computational system [3], [12], [13].

A critical component of cognitive radio networks is energy detection. When there is significant channel fading, though, it performs poorly and interferes with the primary users. An intelligent reflecting surface (IRS)-enhanced energy detection for spectrum sensing is essential to address this problem. The central limit theorem and the Gamma distribution approximation are used to generate the closed-form equations for the average probability of detection [14], [15], .

When there are obstructions blocking, spectrum sensing has poor detection performance. As a result, fusion techniques based on cooperative spectrum sensing can be improved by intelligent reflecting surfaces (IRS). Spectrum sensing is an essential front-end technology in a cognitive radio network. It is used to track spectrum weak points and monitor the occupancy state of the spectrum. An individual can sense the spectrum in three significant ways: energy detection, matching filter detection, and feature detection. Since energy detection is a form of blind sensing technology and has the lowest complexity, it has a high study value in the spectrum sensing field [16].

Intelligent reflecting surfaces (IRS) have been shown to improve wireless device performance in propagation scenarios, according to a recent study [17] that was founded on earlier research. The study looks into cognitive radio's spectrum sensing skills in situations where *the IRS aids wireless propagation*. The authors explore the energy detection performance in an IRS-aided propagation context, emphasizing the importance of the problem. They use SNR statistics with the central limit theorem.

In addition to endorsing the work done by [17], researchers in [18] also stressed the significance of SNR as a calibrating parameter and the fading of communication channels. They strive to find solutions for communication problems arising in cognitive radio networks between primary and secondary users. According to experts, a new study indicates that Intelligent Reflecting Surfaces (IRS) may be able to control the propagation channel of wireless devices. IRS impacts cognitive radio networks' spectrum sensing because it alters the channel. The work in [18] demonstrates the usefulness of employing IRS, and its computer simulations, which indicate that the RIS and relaying technologies significantly improve the achievable rate and error performance when used with other devices. Such work is also mentioned in [19], and [20].

Researchers in [21] looked at cognitive radio as a crucial enabling method that gives vital information on spectrum availability is spectrum sensing. Their work is based on the assumption that the primary user (PU) signals received at the cognitive radio (CR) or secondary user (SU) may be practically too weak for accurate detection due to significant wireless channel fading and route loss. They addressed the problem by proposing a novel intelligent reflecting surface (IRS)-assisted spectrum sensing technique for CR.

In [22], researchers examined reconfigurable intelligent surface devices. They considered the cognitive cycle and concluded that spectrum sensing plays the most significant function in cognitive radio-based dynamic spectrum management. According to research in [22], reconfigurable smart surfaces have much potential to enable smart radio environments because they enhance spectrum management and signal coverage. The work in [23] validated the hypotheses in [22] and considered the quantity of components required to attain optimal signal detection. This should lessen the high demand for broadband services and the dispersion of spectrum resources. The researchers in [23] concluded that cognitive radio might be able to address the lack of available spectrum.

The study is validated by [24], which supports the idea that intelligent reflecting surfaces (IRS) can improve the performance of wireless systems in various signal propagation scenarios. The study in [24] concentrated on applying a statistical model that also took SNR into account to assess cognitive radio's spectrum-sensing capabilities in wireless environments enhanced by IRS technology.

In [25], the SNR factor is also connected to IRS and sensor networks. The study concentrated on the one-degree-of-freedom chi-square distribution of signal-to-noise ratio (SNR) in wireless systems with fixed transmit power that use intelligent reflecting surfaces (IRS). IRS can be used in the cognitive radio secondary network, where the secondary source adjusts its power to cause little interference at the primary destination. The study covered SNR and adaptive systems in connection to IRS. [26], which addresses power and cost and examines an IRS-assisted integrated sensing and communication system, further bolsters the findings.

Spectrum sensing-based cognitive radio networks (CRNs) are also discussed in [27], with the mention that intelligent wireless communication systems aim to better use the available frequency spectrum. The work looked at noise, which affects the energy detection (ED) method due to the nature of noise variation, which affects the detection capability.

Because the IRS changes radio waves, the work in [27] is also backed by [28] and [29] in their study of the IRS's influence on radio waves. The reviewers believed that IRS had significant potential to overcome the shortcomings of traditional antennas and fortify wireless networks going forward. The study further claimed that IRS technology creates a paradigm shift by enhancing network capacity, energy efficiency, and signal coverage.

Researchers looked into next-generation mobile networks expected to stand out for their integration of sensing functionalities. The authors in [30] emphasized the importance of understanding how sensing and communication functionalities interact regarding resource utilization while providing insights and guidelines for developing efficient physical-layer techniques. The authors concluded that this requires researching the tradeoff in current

integrated systems between the user's achievable rate and the detection probability for target monitoring.

The work in [30] is supported by [31] considered IRSs and their potential applications in future wireless communications, where expanding coverage is essential. They believed in the particular case of blocking in line-of-sight-blocked settings. Thus, they considered the Analysis of the matching coverage probability of IRS-assisted communication systems crucial.

Researchers discuss the effectiveness of combining IRS with improved channel quality and dependability in [32]. The researchers claimed that since the development of intelligent reflecting surface (IRS) technology, wireless communication systems have experienced a substantial metamorphosis with promising future developments for enhancing the performance of wireless sensor node-based Internet of Things (IoT) applications. A comprehensive analysis of the functionality of multi-agent IoT monitoring systems driven by IRS was offered in the work. Using probability mode, the researchers concentrated on IRS unit selection criteria. Since cars are thought of as mobile nodes and WSN sensor nodes are fixed in locations, the significance of IRS in wireless communication and channel dependability with non-line-of-sight geometrics is also explored in vehicular applications [33].

The use of reconfigurable intelligent surfaces and intelligent reflecting surface devices for 5G and 6G applications is also covered in [34], [35], [36]. To increase the spectrum efficacy and energy efficiency of next-generation wireless communication systems, researchers saw such devices as a technological tool that could be utilized to reorganize wireless propagation ecosystems—there are many reflecting components cause the surfaces' ability to alter their phase shift effectively.

The key to realizing efficient, ultrafast, and reliable communication is the upcoming 6G wireless communication networks, which are anticipated to link everything, offer full-dimensional wireless coverage, and combine all features to enable full-vertical applications. Intelligent reflecting surfaces (IRS) with wireless environment control capabilities are a viable solution for 6G networks. In particular, using massively adjustable elements, IRS may achieve fine-grained 3-D passive beamforming by intelligently controlling the wavefront, including the phase, amplitude, and frequency.

IRS is thought to be a promising technology that can effectively enhance wireless communication networks' performance by intelligently and adaptively controlling the channel environment using large passive reflecting devices with a competitive advantage in 6G networks, the hardware architecture of IRS, and the new IRS-assisted system paradigm, will adapt to the 6G networks and provide an IoT based application network.

This research carries out a comprehensive analysis of the communication efficiency of IRS devices. The work focuses on spectrum analysis in cognitive radio networks and the detection probability (Pdetection) and how it is affected by noise factor (NF), Signal-to-Noise Ratio (SNR), Probability of False Alarm (Pfalse), and User Traffic (TU). The rest of this paper is divided into introduction, material and methods, results and discussion, conclusions.

II. Materials and Method

This work simulates spectrum sensing in cognitive radio networks under different scenarios using intelligent reflecting surfaces (IRSs). The user traffic intensity (T_{user}), noise factor (N_{factor}), signal-to-noise ratio (SNR), and user traffic are significant parameters that are considered. The study examines how these characteristics affect detection probabilities ($P_{detection}$). It also includes the profit from the IRS. A presentation of the detection probability against SNR under different settings is made.

The process carried out in the simulation is:

a. Determining the noise level through noise factors.
b. Allocating Signal-to-Noise range.
c. Determining a false alarm parameter.
d. Selecting user traffic parameters.
e. Computing path gains for the positioned IRS.
f. Detection probability calculation.

III. Results and Discussion

Tables I shows the simulation results for detection probability ($P_{detection}$), as a result of varying the noise factor (N_{factor}), with false alarm (P_{false}) is set to 0.01, and 20% SNR, and user traffic (T_{user}) is set to three different values {10%, 50%, 90%}.

TABLE I
Relationship between N_{factor} and pdetection for P_{FALSE}=0.01

N_{factor}	T_{user}=10%	T_{user}=50%	T_{user}=100%
	$P_{detection}$		
0.00126	0.80	0.68	0.56
0.00158	0.77	0.65	0.53
0.002	0.74	0.62	0.50
0.0025	0.71	0.59	0.47
0.0032	0.68	0.56	0.44
0.004	0.65	0.53	0.41
0.005	0.62	0.50	0.38
0.0063	0.59	0.47	0.35
0.0079	0.56	0.44	0.32
0.01	0.53	0.41	0.28
0.0126	0.50	0.38	0.25
0.0158	0.47	0.35	0.22
0.02	0.44	0.32	0.19
0.025	0.41	0.28	0.16
0.032	0.38	0.25	0.13
0.04	0.35	0.22	0.10
0.05	0.32	0.19	0.08
0.063	0.28	0.16	0.05
0.079	0.25	0.13	0.04
0.1	0.22	0.10	0.02

From Table I, it is clear that $P_{detection}$ decreases as N_{factor} increases per percentage of T_{user}. Figure 1 compares the three levels of user traffic and how in conjunction with N_{factor} affecting $P_{detection}$.

Figure 1 response can be expressed as in equation (1).

$$P_{detection} = -\lambda log_e(N_F) - \mu \quad (1)$$

Where;

$$\lambda = 0.13$$
$$\mu(Bottom\ Curve) = 0.3$$
$$\mu(Middle\ Curve) = 0.2$$
$$\mu(Top\ Curve) = 0.1$$

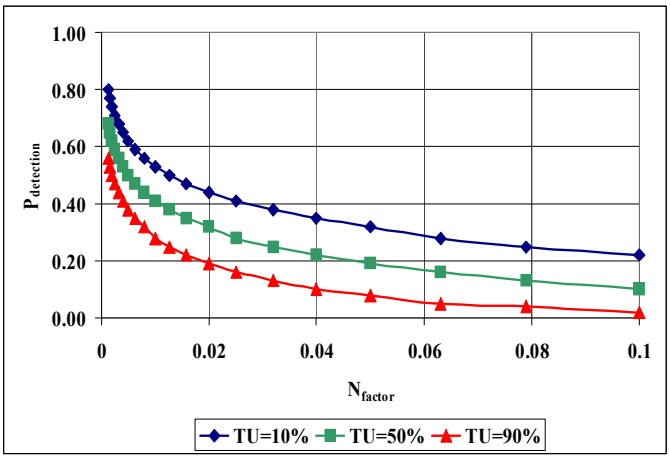

Fig. 1 Relationship between $P_{detection}$ and N_{factor} as a function of T_{user} and P_{false}

Figure 1 shows a decreasing $P_{detection}$ over an SNR range (0 dB to 30 dB) as a function of N_{factor}. A natural logarithmic function describes the response curves. The Figure also shows that response curves are controlled by the T_{user}. This control shifts the curves up or down depending on the level of user traffic experienced by the wireless network. Hence, this can be used as design criteria to enable better probability detection per user traffic.

Figure 2 shows the relationship between average $P_{detection}$ and user traffic. From the Figure, it is clear that as T_{user} increases, $P_{detection}$ decreases. This is due to the accumulative large data, which reduces the efficiency of detection and spectrum sensing. In addition, as shown in Table I, the 0.5 Pdetection occurs at lower SNR values as the T_{user} increases. This is due to increased noise levels, as more users are detected and more communication channels are established.

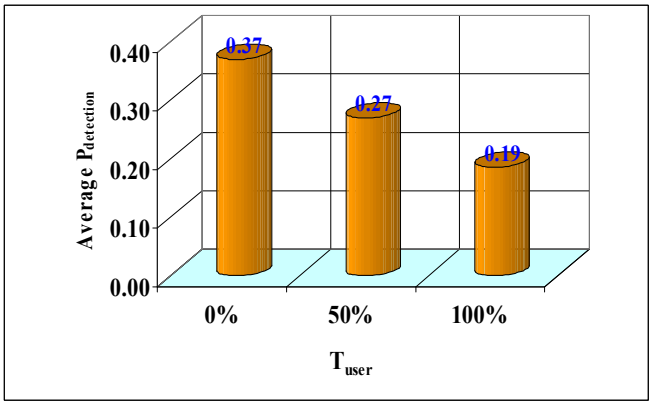

Fig. 2 Relationship between Average $P_{detection}$ and T_{user} as a function of N_{factor} and Pfalse

From Table I, it is also noticeable that the noise factor ratio (0.5 $P_{detection}$) at 10% user traffic to 50% user traffic is 0.25, and the ratio of the Nfactor at 50% Tuser to 90% Tuser is 2.5. This is a good indication of the network spectrum sensing and its relation to Tuser, which is related to SNR, as data traffic and the level of noise are increasing.

Table II presents simulation results relating T_{user} variation to $P_{detection}$ as N_{factor} increases, and for a constant P_{false}.

TABLE II
RELATIONSHIP BETWEEN T_{USER} AND $P_{DETECTION}$ FOR P_{FALSE}=0.01

T_{user}	N_{factor}=0.00126	N_{factor}=0.00316	N_{factor}=0.01
	$P_{detection}$		
10	0.80	0.68	0.56
20	0.77	0.65	0.53
30	0.74	0.62	0.50
40	0.71	0.59	0.47
50	0.68	0.56	0.44
60	0.65	0.53	0.41
70	0.62	0.50	0.38
80	0.59	0.47	0.35
90	0.56	0.44	0.32

Figure 3 shows the relationship between N_{factor} and $P_{detection}$ as a function of increasing T_{user}.

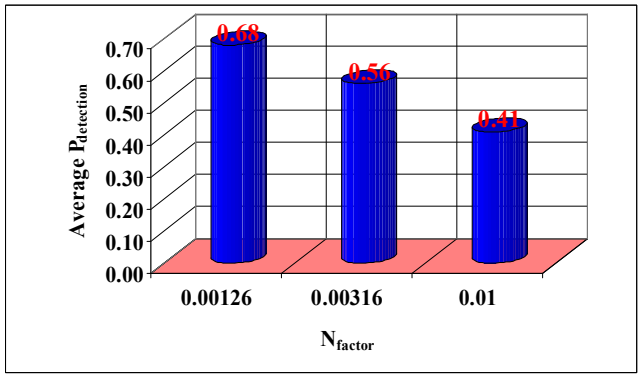

Fig. 3 Relationship between Average $P_{detection}$ and N_{factor} as a function of T_{user} for P_{false}=0.01

From Figure 3, it is clear that as the noise factor increases for a fixed probability of false alarm, and with user traffic increase, detection probability decreases, with a reducing average. This is related to the relationship between noise factor and SNR as described in equation (2).

$$N_{factor} = \frac{\left({Signal_{input}}/{Noise_{input}}\right)}{\left({Signal_{output}}/{Noise_{output}}\right)} \quad (2)$$

Equation (2) can be simplified as in equation (3).

$$N_{factor} = \frac{(SNR_{in})}{(SNR_{out})} \quad (3)$$

The noise figure (F) is given as in equation (4).

$$F\ (dB) = 10 * log(N_{factor}) \quad (4)$$

The N_{factor} is the measure of deterioration of the signal to noise ratio during communication in the wireless network. Since the signal to noise ratio at the output will always be lower than the Signal to Noise ratio at the input, N_{factor} is always less than 1. With clear indication from equation (2) that lower the N_{factor} value, results in better device performance and higher detection probability and spectrum sensing.

Table III shows the relationship between P_{false} and $P_{detection}$ as a function of increasing N_{factor} for a %10 T_{user}. Table III shows that as P_{false} increases, $P_{detection}$ also increases within an N_{factor} dimension. The second dimension is the reduction of $P_{detection}$ as N_{factor} increases.

TABLE III
RELATIONSHIP BETWEEN N_{FACTOR} AND $P_{DETECTION}$ FOR T_{USER}=10%

P_{false}	N_{factor}=0.00126	N_{factor}=0.00316	N_{factor}=0.01
	$P_{detection}$		
0.01	0.80	0.68	0.53
0.02	0.83	0.72	0.56
0.03	0.85	0.74	0.59
0.04	0.86	0.75	0.61
0.05	0.87	0.77	0.62
0.06	0.88	0.78	0.64
0.07	0.89	0.79	0.65
0.08	0.90	0.80	0.66
0.09	0.90	0.81	0.67
1.00	0.91	0.82	0.68

However, it is noticeable from Figure 4 that the average $P_{detection}$, which is a function of both an increase in P_{false}, and a function of N_{factor} is higher than that presented in Figure 3, which is a function of T_{user} and N_{factor}. This is logical, as $P_{detection}$ values are higher for higher P_{false}, while $P_{detection}$ values decrease as a function of T_{user}.

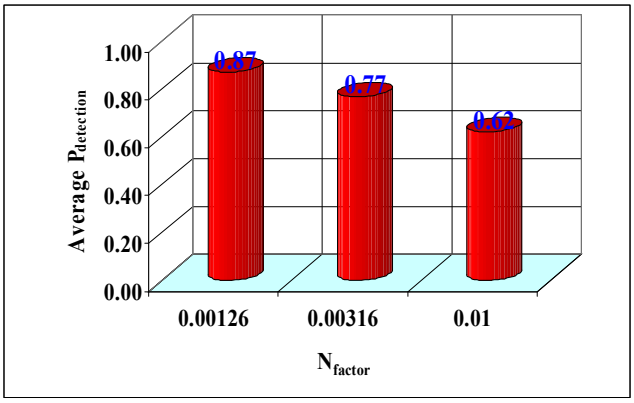

Fig. 4 Relationship between Average $P_{detection}$ and N_{factor} as a function of P_{false} for T_{user}=10%.

Table IV shows the relationship between P_{false} and $P_{detection}$ as a function of increasing N_{factor} for a 50% T_{user}.

TABLE IV
RELATIONSHIP BETWEEN N_{FACTOR} AND $P_{DETECTION}$ FOR T_{USER}=50%

P_{false}	N_{factor}=0.00126	N_{factor}=0.00316	N_{factor}=0.01
	$P_{detection}$		
0.01	0.68	0.56	0.41
0.02	0.72	0.59	0.44
0.03	0.74	0.62	0.46
0.04	0.75	0.64	0.48
0.05	0.77	0.65	0.50
0.06	0.78	0.67	0.51
0.07	0.79	0.68	0.53
0.08	0.80	0.69	0.54
0.09	0.81	0.70	0.55
1.00	0.82	0.71	0.56

Table IV shows that as P_{false} increases, so does $P_{detection}$. Figure 5 shows that the average $P_{detection}$ decreases with increasing N_{factor}, but increases as P_{false} increases (In comparison with Figure 3). However, as $P_{detection}$ decreases with the increase in T_{user}, the values in Figure 5 are less than those in Figure 4, as T_{user} is increased to 50%.

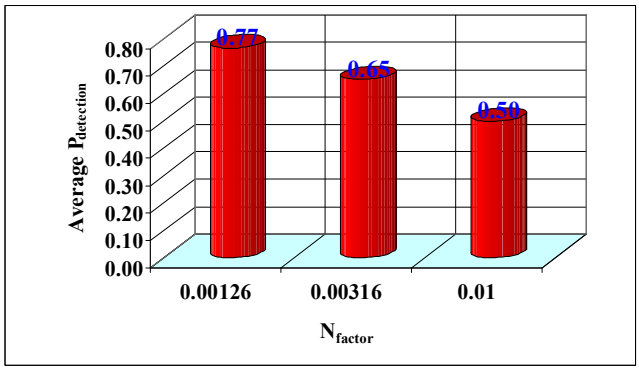

Fig. 5 Relationship between Average $P_{detection}$ and N_{factor} as a function of P_{false} for T_{user}=50%.

Table V shows the relationship between P_{false} and $P_{detection}$ as a function of increasing noise factor for a 90% T_{user}.

TABLE V
RELATIONSHIP BETWEEN N_{FACTOR} AND $P_{DETECTION}$ FOR T_{USER}=90%

P_{false}	N_{factor}=0.00126	N_{factor}=0.00316	N_{factor}=0.01
	$P_{detection}$		
0.01	0.56	0.44	0.28
0.02	0.59	0.47	0.31
0.03	0.62	0.49	0.34
0.04	0.61	0.51	0.36
0.05	0.65	0.53	0.37
0.06	0.67	0.54	0.39
0.07	0.68	0.56	0.40
0.08	0.69	0.57	0.41
0.09	0.70	0.58	0.42
0.1	0.71	0.59	0.44

The results in Table V shows that as P_{false} increases, so does the $P_{detection}$. Figure 6 shows that the average $P_{detection}$ decreases with increasing N_{factor}, but increases as P_{false} increases (In comparison with Figure 3). However, as $P_{detection}$ decreases with the increase in T_{user}, the values in Figure 6 are less than those in Figures 4 and 5, as T_{user} is increased to 90%.

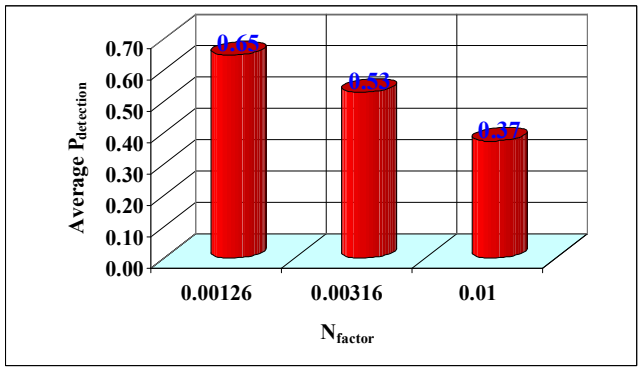

Fig. 6 Relationship between Average $P_{detection}$ and N_{factor} as a function of P_{false} for T_{user}=90%.

The previous results indicate that there should be a balance in T_{user} with N_{factor} in order to optimize $P_{detection}$ and reduce the effect of P_{false} in spectrum sensing. This will make the network communication system more robust and reliable, with the IRS having its most effect on improving communication links and communication efficiency.

Table VI shows a comparison between $P_{detection}$ values as a function of both N_{factor} and T_{user}. From the Table VI, it is clear that as T_{user} and N_{factor} increase, $P_{detection}$ decreases. In addition, there is some kind of symmetry in the listed values, if considered as a matrix. The diagonal values (approximately 0.6), separate the high $P_{detection}$ both the high level (0.77), and low level (approximately 0.5). Closer look at the distributed values shows that there is a difference of 0.5 between the highest $P_{detection}$ and the lowest one. This enables characterization of the IRS wireless communication system response.

TABLE VI
RELATIONSHIP BETWEEN P_{FALSE} AND $P_{DETECTION}$ AS A FUNCTION OF T_{USER}

N_{factor}	$P_{detection}$		
	T_{user}		
	10%	50%	90%
0.00126	0.56	0.44	0.28
0.00136	0.59	0.47	0.31
0.01	0.62	0.49	0.34

Table VII shows the simulation results for $P_{detection}$, as a result of varying N_{factor}, with P_{false} is set to 0.01, and 80% SNR, and T_{user} is set to three different values {10%, 50%, 90%}.

TABLE VII
RELATIONSHIP BETWEEN N_{FACTOR} AND $P_{DETECTION}$ FOR P_{FALSE}=0.01 AND 80% SNR

N_{factor}	T_{user}=10%	T_{user}=50%	T_{user}=100%
	$P_{detection}$		
0.00126	0.87	0.79	0.72
0.00158	0.85	0.77	0.70
0.002	0.83	0.76	0.68
0.0025	0.81	0.74	0.66
0.0032	0.79	0.72	0.64
0.004	0.77	0.70	0.62
0.005	0.76	0.68	0.60
0.0063	0.74	0.66	0.58
0.0079	0.72	0.64	0.56
0.01	0.70	0.62	0.54
0.0126	0.68	0.60	0.52
0.0158	0.66	0.58	0.50
0.02	0.64	0.56	0.48
0.025	0.62	0.54	0.46
0.032	0.60	0.52	0.44
0.04	0.58	0.50	0.42
0.05	0.56	0.48	0.40
0.063	0.54	0.46	0.38
0.079	0.52	0.44	0.36
0.1	0.50	0.42	0.34

Comparing Table VII with Table I, shows that the 0.5 $P_{detection}$ values occurs at higher levels of N_{factor}. This is due to the increase in IRS gain as a result of the increase in the SNR from 20% to 80%. Figure 7 shows a decreasing $P_{detection}$ over an SNR range (0 dB to 30 dB) as a function of N_{factor}. A natural logarithmic function describes the response curves. The Figure also shows that response curves are controlled by T_{user}. Comparing the responses in Figure 7 with the ones in Figure 1, shows that the plots in Figure 7 are closer to each other with higher values associated with the increase in SNR from 20% to 80%, which affected the IRS gain and resulted in a reverse in mathematical model coefficients as shown in equation (5).

$$P_d = -\alpha log_e(N_F) + \beta \quad (5)$$

Where;

$$P_d = \alpha = 0.9$$
$$\beta(Bottom\ Curve) = 0.15$$
$$\beta(Middle\ \ Curve) = 0.2$$
$$\beta(Top\ Curve) = 0.3$$

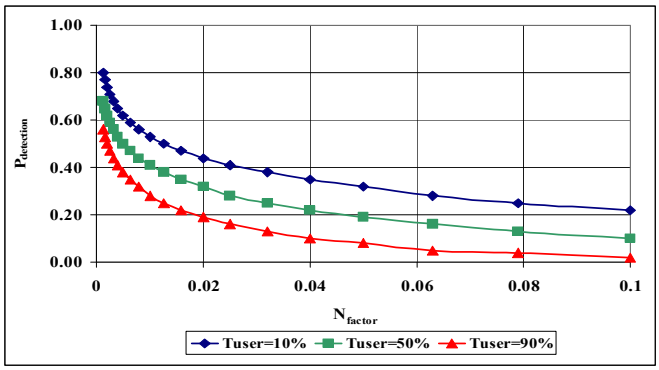

Fig. 7 Relationship between Pdetection and Nfactor as a function of Tuser and Pfalse (80% SNR)

Figure 8 shows the relationship between average $P_{detection}$ and T_{user} for both 20% SNR and 80% SNR. From the Figure, it is clear that as the percentage of SNR increases, so does $P_{detection}$. Although, for a specific SNR range, $P_{detection}$ decreases as a function of T_{user}.

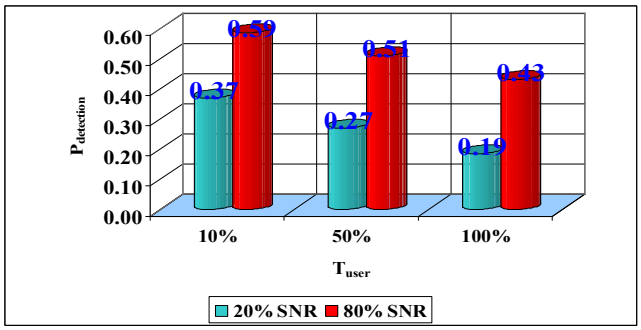

Fig. 8 Comparison between 20% SNR and 80% SNR of Relationship between Average $P_{detection}$ and N_{factor} as a function of P_{false} for T_{user}=10%.

Table VIII presents simulation results relating T_{user} variation to $P_{detection}$ as N_{factor} increases, and for a constant P_{false} for 80% SNR, with Figure 9 showing a comparison between 20% SNR and 80% SNR $P_{detection}$ as a function of T_{user} at 0.01 P_{false}.

TABLE VIII
RELATIONSHIP BETWEEN T_{USER} AND $P_{DETECTION}$ FOR P_{FALSE}=0.01, SNR 80%

T_{user}%	N_{factor}=0.00126	N_{factor}=0.00316	N_{factor}=0.01
	$P_{detection}$		
10	0.87	0.79	0.70
20	0.85	0.77	0.68
30	0.83	0.76	0.66
40	0.81	0.74	0.64
50	0.79	0.72	0.62
60	0.77	0.70	0.60
70	0.76	0.68	0.58
80	0.74	0.66	0.56
90	0.72	0.64	0.54

Figure 9 shows that $P_{detection}$ is less affected by T_{user} at 80% SNR compared to 20% SNR. Table IX shows that as P_{false} increases, $P_{detection}$ also increases much more for 80% SNR compared to Table III, within a noise factor dimension.

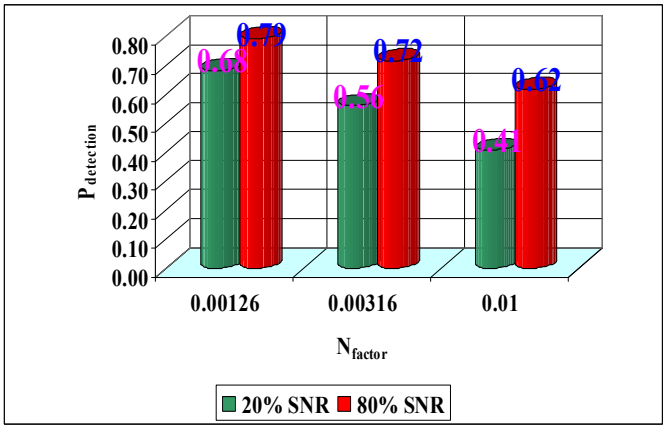

Fig. 9 Comparison between 20% SNR and 80% SNR for Relationship between Average $P_{detection}$ and N_{factor} as a function of T_{user} for P_{false}=0.01

TABLE IX
RELATIONSHIP BETWEEN P_{FALSE} AND $P_{DETECTION}$ FOR T_{USER}=10%, 80% SNR

P_{false}	N_{factor}=0.00126	N_{factor}=0.00316	N_{factor}=0.01
	$P_{detection}$		
0.01	0.87	0.79	0.70
0.02	0.89	0.81	0.72
0.03	0.90	0.83	0.73
0.04	0.91	0.84	0.75
0.05	0.92	0.85	0.76
0.06	0.92	0.86	0.77
0.07	0.93	0.86	0.78
0.08	0.93	0.87	0.78
0.09	0.93	0.88	0.79
0.1	0.94	0.88	0.80

Figure 10 shows a comparison $P_{detection}$ at 20% SNR and 80% SNR, with the values at 80% are higher as expected. The dimension of $P_{detection}$ reduction as N_{factor} increases is also evident for both cases.

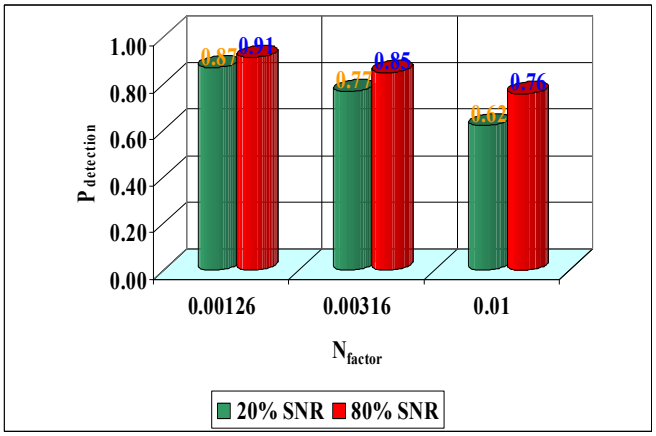

Fig. 10 Relationship between $P_{detection}$ and N_{factor} as a function of T_{user} and P_{false} (80% SNR)

Table X shows the relationship between P_{false} $P_{detection}$ as a function of increasing N_{factor} for a 50% user traffic and 80% SNR, with Figure 11 showing a comparison between 20% SNR and 80% SNR.

TABLE X
RELATIONSHIP BETWEEN P_{FALSE} AND $P_{DETECTION}$ FOR T_{USER}=50%

P_{false}	N_{factor}=0.00126	N_{factor}=0.00316	N_{factor}=0.01
	$P_{detection}$		
0.01	0.79	0.72	0.62
0.02	0.81	0.74	0.64
0.03	0.83	0.75	0.66
0.04	0.84	0.77	0.67
0.05	0.85	0.78	0.68
0.06	0.86	0.79	0.69
0.07	0.86	0.79	0.70
0.08	0.87	0.80	0.71
0.09	0.88	0.81	0.72
0.1	0.88	0.82	0.72

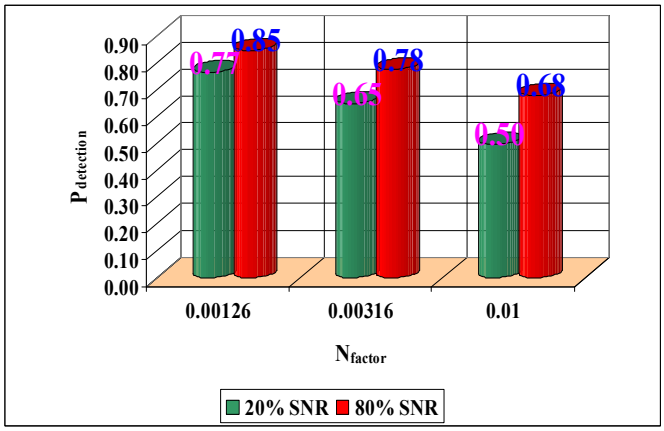

Fig. 11 Comparison between 20% SNR and 80% SNR for the Relationship between Average $P_{detection}$ and N_{factor} as a function of P_{false} for T_{user}=50%.

Table XI shows that as P_{false} increases, so does the $P_{detection}$. Figure 11 shows that the average $P_{detection}$ at 80% SNR is higher than that at 20% SNR, but both suffer reduction with increasing N_{factor}. Table XI shows the relationship between P_{false} and $P_{detection}$ as a function of increasing N_{factor} for a 90% T_{user} and 80% SNR.

TABLE XI
RELATIONSHIP BETWEEN P_{FALSE} AND $P_{DETECTION}$ FOR T_{USER}=90% , 80% SNR

P_{false}	N_{factor}=0.00126	N_{factor}=0.00316	N_{factor}=0.01
	$P_{detection}$		
0.01	0.72	0.64	0.54
0.02	0.74	0.66	0.56
0.03	0.75	0.68	0.58
0.04	0.77	0.69	0.59
0.05	0.78	0.70	0.60
0.06	0.79	0.71	0.61
0.07	0.79	0.72	0.62
0.08	0.80	0.73	0.63
0.09	0.81	0.74	0.64
0.1	0.82	0.74	0.65

The results in Table XII shows that as P_{false} increases, so does $P_{detection}$. This is true for both 20% SNR and 80% SNR. Figure 12 shows that $P_{detection}$ is still higher at 90% traffic for 80% SNR compared to 20% SNR.

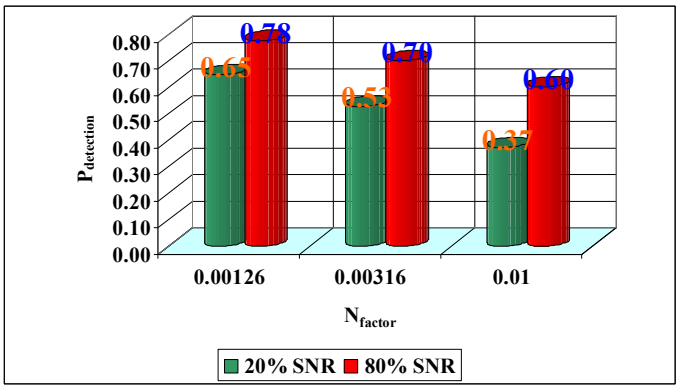

Fig. 12 Comparison between 20% SNR and 80% SNR for the Relationship between Average $P_{detection}$ and N_{factor} as a function of P_{false} for T_{user}=90%.

A comparison of $P_{detection}$ values as a function of T_{user} and N_{factor} is presented in Table XII. The table makes it evident that $P_{detection}$ drops as T_{user} and N_{factor} rise. Furthermore, when viewed as a matrix, the mentioned values exhibit some symmetry. Approximately 0.8 is the diagonal value that divides the high $P_{detection}$ from the low $P_{detection}$. The low level (approximately 0.7) and high level (0.85) both exhibit symmetry. A closer examination of the dispersed numbers reveals that the top and lowest detection probabilities differ by about 0.3. As a result, characterization of the IRS wireless communication system response is made possible.

TABLE XII
RELATIONSHIP BETWEEN P_{FALSE} AND $P_{DETECTION}$ AS A FUNCTION OF T_{USER} FOR 80% SNR

N_{factor}	$P_{detection}$		
	T_{user}		
	10%	50%	90%
0.00126	0.91	0.85	0.78
0.00316	0.85	0.78	0.70
0.01	0.76	0.68	0.60

Tables XIII shows the simulation results for $P_{detection}$, as a result of varying the N_{factor} with P_{false} is set to 0.01, and 80% SNR, and T_{user} is set to three different values {10%, 50%, 90%}. The results simulates variable environmental conditions and instability of communication. Figure 13 shows a comparison, with the responses for unstable conditions having lower values compared to the stable ones. This is logical, as instability negatively affects spectrum sensing.

TABLE XIII
RELATIONSHIP BETWEEN N_{FACTOR} AND $P_{DETECTION}$ FOR P_{FALSE}=0.01 AND 80% SNR AND VARIABLE ENVIRONMENT CONDITIONS

N_{factor}	T_{user}=10%	T_{user}=50%	T_{user}=100%
	$P_{detection}$		
0.00126	0.80	0.75	0.64
0.00158	0.79	0.66	0.64
0.002	0.77	0.68	0.65
0.0025	0.79	0.66	0.57
0.0032	0.74	0.66	0.57
0.004	0.73	0.66	0.60
0.005	0.70	0.58	0.61
0.0063	0.71	0.66	0.53
0.0079	0.64	0.60	0.53
0.01	0.67	0.55	0.52
0.0126	0.65	0.57	0.43
0.0158	0.60	0.55	0.44
0.02	0.59	0.50	0.45
0.025	0.59	0.51	0.45
0.032	0.54	0.43	0.42
0.04	0.53	0.46	0.38
0.05	0.42	0.42	0.30
0.063	0.50	0.42	0.30
0.079	0.45	0.39	0.28
0.1	0.47	0.38	0.27

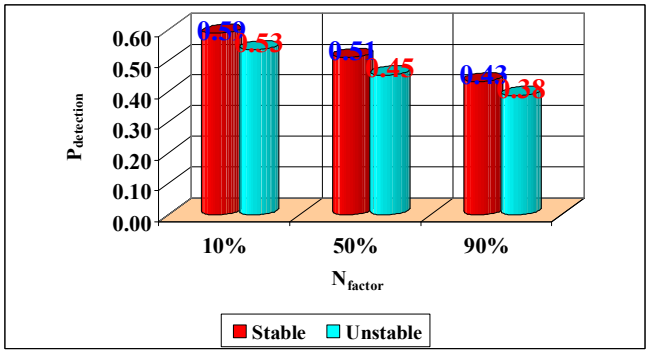

Fig. 13 Comparison between stable and unstable spectrum sensing for the Relationship between Average $P_{detection}$ and N_{factor} as a function of P_{false}.

Figure 14 shows the characteristics and effect of instability on the responses signals, as a function of N_{factor} for a range of user traffic.

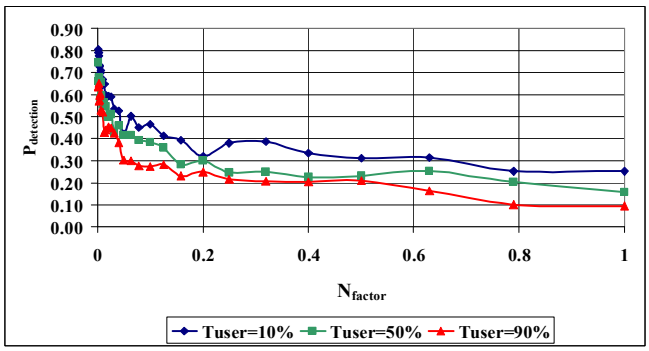

Fig. 14 Relationship between $P_{detection}$ and N_{factor} as a function of T_{user} and P_{false} under unstable conditions.

IV. CONCLUSION

The IRS, or intelligent reflecting surface, exhibits significant potential for use in wireless networks. IRS dynamically modifies the reflection amplitudes and phase shifts of many devices to enable flexible wireless channel control and configuration. The wireless signal's reliability and transmission rate are significantly increased as a result. Spectrum sensing and communication security are essential elements of cognitive radio networks. The precision of spectrum sensing and security performance can be simultaneously enhanced by intelligent reflecting surfaces (IRS). This work computes the detection probability ($P_{detection}$) of an IRS-based wireless system and uses MATLAB simulation to analyze the impact of user traffic (T_{user}), noise factor (N_{factor}), and likelihood of false alarm (P_{false}) on the system's capacity to sense the spectrum. Results, an analysis, and a mathematical model is provided, which describes the response and ability to detect and sense cognitive radio

spectrum under both stable and unstable conditions, and under different noise and user traffic situations. Furthermore, two levels of Signal-to-Noise Ratio (SNR)—20% and 80% noise—are considered. This makes it possible to evaluate spectrum sensing in various scenarios. According to the data, $P_{detection}$ declines with a logarithmic form function as N_{factor} rises per percentage of T_{user}. The investigation also reveals that when the user traffic level rises above 50%, the noise factor increases tenfold. For a certain probability of false alarm, the noise factor rises, user traffic increases, detection probability falls, and P_{false} increases along with Pdetection. According to the results, T_{user} and N_{factor} should be balanced to maximize $P_{detection}$ and minimize $P_{false's}$ impact on spectrum sensing. This can be achieved, by optimizing the communication channel and its capacity to enable less noisy signals, which enables higher bit rate with lower false alarms probability, and higher probability of detection. The provision of better channel capacity, which is dependent on SNR, is a key factor in enabling lower false alarms and better detection probability. In addition, with adaptive IRS and more intelligent control, higher traffic and lower noise factor is achieved.

Future work should consider number of elements per IRS devices that could lead to more efficient communication and better spectrum detection. Also, using large number of elements per IRS, enable higher user traffic with better channel optimization and wider tolerance to the presence of noise.

ACKNOWLEDGMENT

The simulation software is based on code originally written by Ardavan Rahimian and has been modified for the purpose of this work. No research fund is obtained for this work.

REFERENCES

[1] Z. Chu, Z. Zhu, F. Zhou, M. Zhang, and N. Al-Dhahir, "Intelligent reflecting surface assisted wireless powered sensor networks for Internet of Things," *IEEE Trans. Commun.*, vol. 69, no. 7, pp. 4877–4889, Jul. 2021, doi: 10.1109/tcomm.2021.3074539.

[2] W. Mei, B. Zheng, C. You, and R. Zhang, "Intelligent reflecting surface-aided wireless networks: From single-reflection to multireflection design and optimization," *Proc. IEEE*, vol. 110, no. 9, pp. 1380–1400, Sep. 2022, doi: 10.1109/jproc.2022.3170656.

[3] D. Pérez-Adán, Ó. Fresnedo, J. P. Gonzalez-Coma, and L. Castedo, "Intelligent reflective surfaces for wireless networks: An overview of applications, approached issues, and open problems," *Electronics*, vol. 10, no. 19, p. 2345, Oct. 2021, doi: 10.3390/electronics10192345.

[4] Y. Wang, B. Ji, and D. Li, "IRS assist wireless communication: Scenarios, advantages, convergence," *J. Comput. Electron. Inf. Manag.*, vol. 10, no. 3, pp. 40–45, 2023, doi: 10.54097/jceim.v10i3.8679.

[5] O. Bouhamed, H. Ghazzai, H. Besbes, and Y. Massoud, "A UAV-assisted data collection for wireless sensor networks: Autonomous navigation and scheduling," *IEEE Access*, vol. 8, pp. 110446–110460, 2020, doi: 10.1109/access.2020.3002538.

[6] Z. Zhang, W. Chen, Q. Wu, Z. Li, X. Zhu, and J. Chen, "Multiple intelligent reflecting surfaces collaborative wireless localization system," *IEEE Trans. Wireless Commun.*, vol. 24, no. 1, pp. 134–148, Jan. 2025, doi: 10.1109/twc.2024.3488822.

[7] K. Aswini and M. Surendar, "Performance analyses of intelligent reflecting surface aided downlink multi-user rate-splitting multiple access system for 6G applications," *Comput. Netw.*, vol. 242, p. 110271, 2024, doi: 10.1016/j.comnet.2024.110271.

[8] V. Srivastava and B. Prasad, "IRS assisted spectrum sensing in cognitive radio network with grey wolf optimization," *Phys. Commun.*, vol. 66, p. 102436, 2024, doi: 10.1016/j.phycom.2024.102436.

[9] L. Al-Zabin, O. Al-Wesabi, H. Al Hajri, N. Abdullah, B. Khudayer, and H. Al Lawati, "Probabilistic detection of indoor events using a wireless sensor network-based mechanism," *Sensors*, vol. 23, no. 15, p. 6198, 2023, doi: 10.3390/s23156198.

[10] S. Sur and R. Bera, "Intelligent reflecting surface assisted MIMO communication system: A review," *Phys. Commun.*, vol. 47, p. 101386, 2021, doi: 10.1016/j.phycom.2021.101386.

[11] W. Tan, Q. Zhou, W. Tan, L. Yang, and C. Li, "Performance analysis of intelligent reflecting surface assisted wireless communication system," *Comput. Model. Eng. Sci.*, vol. 137, no. 1, pp. 775–787, 2023, doi: 10.32604/cmes.2023.027427.

[12] Z. Wang, W. Wu, F. Zhou, B. Wang, Q. Wu, T. Quek, and C. Byoung, "IRS-enhanced spectrum sensing and secure transmission in cognitive radio networks," *IEEE Trans. Wireless Commun.*, vol. 23, no. 8, pp. 10271–10286, Aug. 2024, doi: 10.1109/twc.2024.3370812.

[13] B. Zheng, X. Xiong, T. Ma, J. Tang, D. Ng, and A. Swindlehurst, "Intelligent reflecting surface-enabled anti-detection for secure sensing and communications," *IEEE Wireless Commun.* (Early Access), 2025, doi: 10.1109/mwc.006.2400129.

[14] W. Wu, Z. Wang, L. Yuan, F. Zhou, F. Lang, and B. Wang, "IRS-enhanced energy detection for spectrum sensing in cognitive radio," *IEEE Wireless Commun. Lett.*, vol. 10, no. 10, pp. 2254–2258, Oct. 2021, doi: 10.1109/lwc.2021.3099121.

[15] K. Aswini and M. Surendar, "Capacity analysis of intelligent reflecting surface assisted RSMA system with perfect and imperfect CSI for 6G," *J. Phys.: Conf. Ser.*, vol. 2466, no. 1, p. 012001, 2023, doi: 10.1088/1742-6596/2466/1/012001.

[16] G. Peng and W. Wu, "Fusion schemes based on IRS-enhanced cooperative spectrum sensing for cognitive radio networks," *Electronics*, vol. 11, no. 16, p. 2533, 2022, doi: 10.3390/electronics11162533.

[17] R. Kumar and S. Singh, "Intelligent reflecting surface framework for ED based spectrum sensing," *Int. J. Wirel. Inf. Networks*, vol. 31, no. 2, pp. 155–162, 2024, doi: 10.1007/s10776-024-00619-z.

[18] I. Yildirim, F. Kilinc, E. Basar, and G. Alexandropoulos, "Hybrid RIS-empowered reflection and decode-and-forward relaying for coverage extension," *IEEE Commun. Lett.*, vol. 25, no. 5, pp. 1692–1696, May 2021, doi: 10.1109/lcomm.2021.3054819.

[19] R. Alhamad, "Spectrum sensing using intelligent reflecting surfaces with multi-antennas energy harvesting," *Wirel. Pers. Commun.*, vol. 135, pp. 1103–1116, 2024, doi: 10.1007/s11277-024-11110-6.

[20] R. Alhamad, "Cognitive radio networks using intelligent reflecting surfaces," *Comput. Syst. Sci. Eng.*, vol. 43, no. 2, pp. 751–765, 2022, doi: 10.32604/csse.2022.021932.

[21] S. Lin, B. Zheng, F. Chen, and R. Zhang, "Intelligent reflecting surface-aided spectrum sensing for cognitive radio," *IEEE Wireless Commun. Lett.*, vol. 11, no. 5, pp. 928–932, May 2022, doi: 10.1109/lwc.2022.3149834.

[22] M. Saber et al., "Reconfigurable intelligent surfaces improved spectrum sensing in cognitive radio networks," *Procedia Comput. Sci.*, vol. 207, pp. 4113–4122, 2022, doi: 10.1016/j.procs.2022.09.474.

[23] H. Tran and B. Lee, "Enhancing reconfigurable intelligent surface-enabled cognitive analysis and parameter optimization," *Sensors*, vol. 24, no. 15, p. 4869, 2024, doi: 10.3390/s24154869.

[24] R. Kumar, S. Singh, S. Chauhan, A. Anand, and A. Kumar, "ED based spectrum sensing over IRS-assisted Rayleigh-FTR fading channels," *AEU - Int. J. Electron. Commun.*, vol. 171, p. 154908, 2023, doi: 10.1016/j.aeue.2023.154908.

[25] R. Alhamad and H. Boujemaa, "Intelligent reflecting surfaces with adaptive transmit power for underlay cognitive radio networks," *Wirel. Commun. Mobile Comput.*, vol. 2022, p. 2787466, 2022, doi: 10.1155/2022/2787466.

[26] A. Elbir, K. Mishra, M. Shankar, and S. Chatzinotas, "The rise of intelligent reflecting surfaces in integrated sensing and communications paradigms," *IEEE Netw.*, vol. 37, no. 6, pp. 223–241, Nov. 2023, doi: 10.1109/mnet.128.2200446.

[27] J. Lorincz, I. Ramljak, and D. Begušić, "A review of the noise uncertainty impact on energy detection with different OFDM system designs," *Comput. Commun.*, vol. 148, pp. 185–208, 2019, doi: 10.1016/j.comcom.2019.09.013.

[28] K. Felizardo and E. Arboleda, "Next-generation antennas key enabler: Intelligent reflecting surfaces (IRS) technology potential to address limitations of traditional antennas," *Int. J. Sci. Res. Archive*, vol. 12, no. 1, pp. 2608–2613, 2024, doi: 10.30574/ijsra.2024.12.1.1136.

[29] X. Shao, C. You, and R. Zhang, “Intelligent reflecting surface aided wireless sensing: Applications and design issues,” *IEEE Wireless Commun.*, vol. 31, no. 3, pp. 383–389, Jun. 2024, doi: 10.1109/mwc.004.2300058.

[30] J. An, H. Li, D. Ng, and C. Yuen, “Fundamental detection probability vs. achievable rate tradeoff in integrated sensing and communication systems,” *IEEE Trans. Wireless Commun.*, vol. 22, no. 12, pp. 9835–9853, Dec. 2023, doi: 10.1109/twc.2023.3273850.

[31] F. Okogbaa, Q. Ahmed, F. Khan, W. Abbas, S. Zaidi, and T. Alade, “Design and application of intelligent reflecting surface (IRS) for beyond 5G wireless networks: A review,” *Sensors*, vol. 22, no. 7, p. 2436, 2022, doi: 10.3390/s22072436.

[32] Y. Sun, J. Huang, and F. Wei, “Performance evaluation of distributed multi-agent IoT monitoring based on intelligent reflecting surface,” *EURASIP J. Adv. Signal Process.*, vol. 2024, no. 4, 2024, doi: 10.1186/s13634-024-01132-4.

[33] S. Nandan and M. Rahiman, “Intelligent reflecting surface (IRS) assisted mmWave wireless communication systems: A survey,” *J. Commun.*, vol. 17, no. 9, pp. 745–760, 2022, doi: 10.12720/jcm.17.9.745-760.

[34] A. Singh, A. Maurya, R. Prakash, P. Thakur, and B. Tiwari, “Reconfigurable intelligent surface with 6G for industrial revolution: Potential applications and research challenges,” *Paladyn, J. Behav. Robot.*, vol. 14, no. 1, p. 20220114, 2023, doi: 10.1515/pjbr-2022-0114.

[35] M. Sejan, M. Rahman, B. Shin, J. Oh, Y. You, and H. Song, “Machine learning for intelligent-reflecting-surface-based wireless communication towards 6G: A review,” *Sensors*, vol. 22, no. 14, p. 5405, 2022, doi: 10.3390/s22145405.

[36] D. Wang, J. Zhang, and Q. Zhang, “Intelligent reflecting surface-assisted secrecy wireless communication with imperfect CSI,” *Phys. Commun.*, vol. 44, p. 101235, 2021, doi: 10.1016/j.phycom.2020.101235.